ORIGINAL ARTICLE

Influence of extractions on physicochemical characterization and bioactivity of *Piper nigrum* oils: Study on the non-isothermal decomposition kinetic

T. Thanh-Tam Huynh [a,b], Thanh-Chi Mai [b], Chi-Hien Dang [b,c], T. Thuy-Trang Vo [d], Dinh-Truong Nguyen [d,*], Van-Su Dang [e], Khang Duy Vu Nguyen [f], Vinh-Thien Tran [g], Thanh-Danh Nguyen [a,b,*]

[a] *Institute of Research and Development, Duy Tan University, Da Nang City, Viet Nam*
[b] *Institute of Chemical Technology, Vietnam Academy of Science and Technology, Ho Chi Minh City, Viet Nam*
[c] *Graduate University of Science and Technology, Vietnam Academy of Science and Technology, 18 Hoang Quoc Viet, Cau Giay, Hanoi, Viet Nam*
[d] *School of Biotechnology, Tan Tao University, Long An Province, Viet Nam*
[e] *Department of Chemical Technology, Ho Chi Minh City University of Food Industry, Ho Chi Minh, Viet Nam*
[f] *Institute of Applied Material Science, Vietnam Academy of Science and Technology, Ho Chi Minh City, Viet Nam*
[g] *Faculty of Geology & Mineral Resources Engineering, Ho Chi Minh City University of Natural Resources and Environment, Ho Chi Minh City, Viet Nam*

Abstract Black pepper oils have been investigated frequently in the recent years. However, there is a significant variation in physicochemical properties and bioactivity of oils depended on extraction techniques. In this study, the systemic investigation of four various extraction methods was performed to evaluate the physicochemical characterizations, antioxidant and antibacterial activity. The investigation of ^1H NMR, FTIR and UV–Vis spectra confirmed presence of non-volatile components in oils extracted through supercritical CO_2 and hexane-soaking extractions which induced their typical thermal properties. The isothermal behaviour of extracted oils related to evaporation was within range of 3.2–7.3% (w/w) at 27 °C. The SEM images of the black pepper confirmed dif-

* Corresponding authors at: Institute of Chemical Technology, Vietnam Academy of Science and Technology, Ho Chi Minh City, Viet Nam (T. D. Nguyen).
E-mail addresses: truong.nguyen@ttu.edu.vn (D.-T. Nguyen), nguyenthanhdanh3@duytan.edu.vn, danh5463bd@yahoo.com (T.-D. Nguyen).
Peer review under responsibility of King Saud University.

Production and hosting by Elsevier

ferent operation manners of mechanism between extractions using the solvents and heating process. The lowest MIC for both essential oils from conventional hidrodistillation and microwave-assisted hidrodistillation against two bacteria including *E. coli* and *B. subtilis* were found to be 137 μg mL^{-1}. The non-isothermal decomposition kinetics were investigated on the essential oil of microwave-assisted hydrodistillation extraction. The activation energies and pre-exponent factors of non-isothermal decomposition were found to be in range of 36.5–73.7 KJ mol^{-1} and 4.98×10^3–1.97×10^8 s^{-1}, respectively, dependent on conversional fractions of the oil. The results revealed that chemical components, physicochemical properties and bioactivity of black pepper essential oils depended on the extraction techniques.

1. Introduction

Essential oils (EOs) which are defined as secondary metabolites from various organs of plants have long been used in traditional medicine due to therapeutic and preservative properties (Freitas and Cattelan, 2018). The chemical profiles and pharmaceutical properties of EOs can vary in quantity, quality and components according to climate, age of plant, geographical location and extraction methods (Bakkali et al., 2008). Several techniques have been employed to obtain EOs from the aromatic plant such as steam distillation, expression under pressure, supercritical fluid and microwave-assisted extractions, etc. Recent trends have focused on green extraction techniques and toward a cost-effective production of high-quality EOs (Baptista-Silva et al., 2020).

Black pepper, *Piper nigrum* belong to family of Piperaceae is known as an industrial crop species grown popularly in tropical regions including India and South Asia. The black pepper fruits can be used not only for the flavour spice and traditional medicine but also for insecticides and cosmetic industry (Jaramillo and Manos, 2001; Ahmad et al., 2012). The plant is one of the most abundant herbal spices in Vietnam and used as a traditional seasoning. It is inexpensive and available for low socioeconomic population (Kaefer and Milner, 2008; Tran et al., 2019). Thus, the black pepper essential oil (EO) is significantly considered for studies on potential bioactivity (Kamble and Patil, 2008; Sangha et al., 2017; Li et al., 2020). However, its bioactivity is depended on the particular cultivar and the geographical location (Meghwal and Goswami, 2013).

There have been numerous studies on the essential oils of the black pepper fruit. The main compounds presenting in the black pepper oil included piperine, β-pinene, 3-carene, limonene, sabinene and β-caryophyllene have been reported in literature. Content of each components is dependent on the extraction techniques (Bakha et al., 2020; Zhao et al., 2020). Wang and coworkers (2018) reported that the oil from ultrasonic-microwave assisted extraction possessed 3-carene (33%) and limonene (19%) as abundant compounds and their free radical scavenging activity varied by the extraction conditions. Bagheri et al. (2014) have found β-caryophyllene, limonene and sabinene as the major volatile compounds in EOs extracted by hydrodistillation and supercritical CO$_2$ extractions. The antioxidant activity of EO extracted by supercritical CO$_2$ (EC$_{50}$ = 103.3 μg mL^{-1}) was higher than that of hydrodistillation (EC$_{50}$ = 316.2 μg mL^{-1}). Grinevicius and coworkers (2017) reported that the major volatile components of the pepper oils obtained by supercritical CO$_2$ extraction

included piperine (32.1–60.4%), caryophyllene (20.1–45.3%) and β-copaene (4.3–8.9%). There is a significant variation in chemical compositions, physical properties and bioactivity of oils extracted by different techniques. However, the effect of the extraction technique on chemical composition, physical properties and bioactivity of the oils has not been studied systematically so far.

On the other hand, Nisha et al. (2009) have investigated the decomposition kinetics of black pepper flavor at isothermal and non-isothermal conditions using cooking methods at the constant gas flow. This work had important significance in evaluation of temperature influence on the evaporation of the flavor during use of the black pepper as food. In this work, the physicochemical characterizations and bioactivity of the black pepper oils obtained by four different extraction methods including hydrodistillation (HDEO), microwave-assisted hydrodistillation (MAEO), supercritical carbon dioxide (SCEO) and hexane-soaking (HEEO) have been evaluated. The non-isothermal decomposition kinetics of MAEO are investigated by using *iso*-conversional models which were calculated from the TGA data.

2. Experimental

2.1. Plant materials and chemical reagents

Hexane and anhydrous Na$_2$SO$_4$ were purchased from Acros (Belgium). Distilled water was used throughout. Pepper fruits purchased in Ho Chi Minh City were dried in air atmosphere and well grinded with particle size of 0.5–1.0 mm by using an electronic blender.

2.2. Extraction of essential oils

2.2.1. Conventional hydrodistillation
Each sample of ground dry material (100 g) were charged into 1000 mL Clevenger apparatus. Distilled water (500 mL) was added into each sample. The mixture was refluxed for 4 h. The hydrodistilltion essential oil (HDEO) were separated from mixture and dried in anhydrous Na$_2$SO$_4$.

2.2.2. Microwave-assisted hydrodistillation
Microwave-assisted hydrodistillation extraction was performed employing a modified domestic microwave oven, (SANYO EM-G205AW). Dry material (100 g) was added to distilled water (500 mL) into a ground bottom flask-1000 mL

assembled with a Clevenger trap positioned outside. The essential oil (MAEO) were obtained by microwave irradiation at the power level of 500 W for 1 h after dried in anhydrous Na_2SO_4.

2.2.3. Supercritical CO_2 extraction

The supercritical CO_2 method was carried out according to Perakis et al. (2005). Briefly, ground dry material (500 g) was charged into a high pressure vessel (2000 mL) connected with the separators operating up to 200 bar. The extraction was performed at 40 °C and 100 bar in supercritical CO_2 flow rate of 0.5 g/min. After reducing pressure, the CO_2 and essential oil (SCEO) were separated. All EOs were stored at 0–5 °C for further studies.

2.2.4. Hexane extraction

The dry material (100 g) was soaked in n-hexane (300 mL) for 24 h at room temperature. The extract was filtered and HEEO was obtained by concentrating under vacuum at 45 °C.

2.3. GC and GC-MS analysis

Gas chromatography (GC) and Gas chromatography - mass spectrometer (GC-MS) measurements were carried out as previous report (Nguyen et al., 2018). Briefly, the EOs (25 μL) were analyzed on GC (Agilent 6890 N) coupled with HP-5MS Capillary Column (30.0 length × 0.25 mm i.d. × 0.25 μm film thickness). The temperature program was carried out from 50 to 150 °C at the rate of 5 °C min^{-1}, from 150 – 200 °C at the rate of 3 °C min^{-1}, from 200 to 280 °C at the rate of 10 °C min^{-1} and kept at 280 °C for 20 min. The retention index was calculated on the basis of a standard sample containing homologous series of *n*-alkanes (C_8-C_{30}, Sigma Co.). To identify the essential oils, their retention index was compared with the published data (Adams, 2007). For GC analysis, essential oils were also injected to Agilent 6890 N GC with a HP-5MS column fitted with FID detector in conditions equal to GC–MS analysis.

2.4. Measurements

The EOs diluted in hexane were used to measure ultraviolet–visible (UV–Vis) absorption spectra (UV–Vis JASCO V-630 spectrophotometer). A BRUKER EQUINOX 55 IR spectrophotometer was used to measure infrared spectra. ^{1}H NMR (BRUKER AVANCE 500 NMR spectrometer) was recorded by using $CDCl_3$ as solvent and tetramethylsilane (TMS) as internal standard. Thermoanalyzer (TGA/DSC 3 + Mettler-Toledo, USA) was used for simultaneous thermal analysis combining thermogravimetric analysis (TGA) and differential scanning calorimetry (DSC), temperatures range 30–600 °C with a different heating rate in the air flow at 20 mL min^{-1}. Isothermal volatilization of the essential oils utilized TGA measurement in the air flow at 20 mL min^{-1} from 27 °C for 120 min. Surface morphology of the spent pepper solids was evaluated by using a microscope and scanning electron microscope (SEM, S-4800 HI-9057-0006).

2.5. Antioxidant assay

Antioxidant activity of EOs was determined according to 1,1-diphenyl-2-pycrylhydrazile (DPPH) radical scavenging method (Nguyen et al., 2018). Briefly, Four EO samples diluted with different concentrations was mixed with DPPH solution (0.2 mM) in methanol. The mixture then was incubated at room temperature in dark for 20 min and absorbance was measured at 517 nm. Vitamin C (ascorbic acid) purchased from Sigma (USA) was used as a standard antioxidant. Reducing absorbance of the mixture revealed the free radical scavenging. IC_{50} values (μg/mL) which were expressed as the sample concentration required for the half decrease in absorbance of the blank sample was used to evaluate the antioxidant activity of the essential oils.

2.6. Antibacterial assay

The antibacterial activity of EOs was evaluated via the disk diffusion method (Nguyen et al., 2018). A Gram-positive bacterium (*Bacillus subtilis*) and a Gram-negative bacterium (*Escherichia coli*) procured originally from School of Biotechnology, Tan Tao University, Vietnam, were used for biotests. The standard antibiotic ampicillin (0.01 mg/mL) was used as a positive control and Luria Bertani broth was used as a negative control. The inoculated disks were incubated at 37 °C and diameters of inhibition zone around the paper disks in millimeter was recorded after 12 h.

2.7. Non-isothermal decomposition kinetic study

Non-isothermal kinetic of EOs was analysed using isoconversional method. This method based on free models allows the determination of parameters such as activation energy (E_a) and pre-exponential factor (A). The activation energy is identified as energy needed to provide for a chemical reaction to take place (Rueda-Ordóñez and Tannous, 2015). It is also known as the potential barrier to break the bonds among molecules creating an active transition-state complex. The pre-exponential factor is known as the number of collisions per unit time in obtaining the proper orientation to react.

In this work, the sample of MAEO was selected to investigate non-isothermal decomposition kinetics. The thermal decomposition of EO is carried out at varied heating rates (10, 15, 20 and 25 K min^{-1}). Each samples (25 mg) was measured under air atmosphere at a flow rate of 20 mL min^{-1}. The conversional fraction is defined as the mass fraction of degraded sample as shown in the Eq. (1).

$$\alpha = \frac{m_i - m_t}{m_i - m_f} \tag{1}$$

where m_i, m_t and m_f are the initial, instantaneous and final weights of the feed EO sample, respectively. In non-isothermal degradation, the rate expression for conversion of decomposed sample combined with Arrhenius expansion for rate constant can be described using a general form of Eq. (2).

$$\frac{d\alpha}{dt} = Ae^{\frac{-E_a}{RT}}f(\alpha) \tag{2}$$

where f(α) is the reaction model; E_a and A are the activation energy and the pre-exponential factor, respectively; T is the absolute temperature at time t and R is the gas constant. The non-isothermal rate of decomposition from TGA data could be expressed by the Eq. (3).

$$\frac{d\alpha}{dT} = \frac{d\alpha}{dt} \times \frac{dt}{dT} \tag{3}$$

where dα/dT and dα/dt are the non-isothermal and isothermal reaction rates, respectively and dT/dt is the heating rate expressed as variable β. Thus, non-isothermal rate equation of degradation could be derived as the Eq. (4).

$$\frac{d\alpha}{dT} = \frac{A}{\beta} e^{\frac{-E_a}{RT}} f(\alpha) \tag{4}$$

The integral form of reaction model is often used to perform kinetic calculations.

$$g(\alpha) = \int_0^\alpha \frac{d\alpha}{f(\alpha)} = \frac{A}{\beta} \int_0^T e^{\frac{-E_a}{RT}} \tag{5}$$

According to the non-isothermal model free methods, evaluation of activation energy is based on the *iso*-conversional rate which is only dependent on reaction temperature. Thus, the reaction rate at a specific conversional value (α) for a certain heating rate (β) is a function of temperature (T) while model reaction (f(α)) remains unchanged. In this work, two integral *iso*-conversional methods including Flynn-Wall-Ozawa (FWO), Kissinger-Akahira-Sunose (KAS) and a differential *iso*-conversional method namely Friedman were used to determine activation energy of thermal decomposition from the TGA data while Kissinger method was used to calculate values of pre-exponential factor (A).

2.7.1. Integral iso-conversional methods

Flynn-Wall-Ozawa (FWO) method (Flynn, 1997) is obtained by integrating Eq. (5) and implementing Doyle's approximation to the temperature integral (Doyle, 1962).

$$Ln\beta = Ln\left(\frac{A_\alpha R}{E_a g(\alpha)}\right) - 5.331 - 1.052 \frac{E_a}{RT_\alpha} \tag{6}$$

For each corresponding values of α, each pairs of ln β and 1/T data point from four different heating rates were plotted and fitted to a linear model. The values of E_a were consequently calculated from the slope of relating straight lines.

Kissinger-Akahira-Sunose (KAS) method (Akahira and Sunose, 1971) determined E_a values based on approximation given by Murray and White (Murray and White, 1955) via Eq. (7).

$$Ln\left(\frac{\beta}{T_\alpha^2}\right) = Ln\left(\frac{A_\alpha R}{E_a g(\alpha)}\right) - \frac{E_a}{RT_\alpha} \tag{7}$$

Value of E_a could be calculated from Eq. (7) by determining the slope of pairs of ln (β/T²) and 1/T plotted for each corresponding value of α.

2.7.2. Differential iso-conversional methods

Friedman method (Friedman, 1964) is the simplest type of *iso*-conversional method and the most widely used for non-thermal kinetic analysis, derived by taking the logarithm for both sides of Equation (4). The Friedman equation is expressed as follows,

$$Ln\left(\frac{d\alpha}{dt}\right)_\alpha = Ln(A * f(\alpha)) - \frac{E_a}{RT} \tag{8}$$

The combination between (3) and (8) can derive Eq. (9)

$$Ln\left(\beta \frac{d\alpha}{dT}\right)_\alpha = Ln(A * f(\alpha)) - \frac{E_a}{RT} \tag{9}$$

For each corresponding values of α, value of E_a could be calculated from Eq. (9) by determining the slope of pairs of ln (βdα/dT) and 1/T plotted.

2.7.3. Determination of pre-exponential factor

Although the mentioned *iso*-conversional methods could provide an accurate way to calculate E_a, the reaction model or pre-exponential factor (A) of decomposition could not be obtained. Kissinger method was a useful tool to determine both of E_a and A through the equation given as,

$$Ln\left(\frac{\beta}{T_d^2}\right) = Ln\left(\frac{AR}{E_a}\right) - \frac{E_a}{RT_d} \tag{10}$$

where T_d is the temperature peak of DTG curves. Because Kissinger method only conducts a single value of E_a for the overall process, it was not utilized to calculate E_a. However, if the value of E_a were known for each conversional fraction, the value of A could be derived from Eq. (11) as follows,

$$A_\alpha = \frac{\beta E_a \exp\left(\frac{E_a}{RT_d}\right)}{RT_d^2} \tag{11}$$

3. Results and discussion

3.1. Comparative analysis of physicochemical properties

3.1.1. Volatile compositions of essential oils

The components of EOs from different extractions were determined by GC-MS methods. There are significant differences in the yields and the components. The yield of EOs obtained in order of hexane (3.60 ± 0.05%), superficial CO_2 (3.10 ± 0.05%), HD (2.70 ± 0.03%) and MW (2.10 ± 0.03%). In spite of the highest yield of hexane extract, some solids are precipitated during the storage process. It can be due to aggregation of compounds with high molecular mass such as fatty acids and steroids (Hoerr and Harwood, 1951; Peng et al., 2001). The HD and MA extractions obtain EOs with a high volatility. Meanwhile, the advantages of extraction using superficial CO_2 are not only reduced usage of organic solvents with potential risk of storage but obtained a high yield of essential oils with high volatility.

The results of compositional analysis are shown in Table 1. The relative percentage content of compounds was calculated by area integration method from GC and GC-MS data and the results are expressed retention index and percentage values. A total of 25 identifiable volatile compounds are found in all samples. It is clear that the major components identified in *P. nigrum* EOs are dependent on the extraction methods. Hydrocarbons were identified as the abundant composition in all EOs. The content of volatile component that cannot be identified from GC-MS data is the highest in HEEO sample with 16.7% while non-identifiable component in samples MAEO and CSEO is only 1.0% and 0.6%, respectively. GC data of the non-identifiable volatile components in HEEO find at high retention time which can relate to the compounds possessing the high boiling point. The major compounds found in both samples, CSEO and HEEO, are similar to dominate content of sesquiterpenes. CSEO showed β-caryophyllene (48.4%), 3-carene (12.1%), d-limonene (10.8%), β-pinene (5%), copaene (4.8%), δ-3-elemene (4.6%), humulene (2.4%)

Table 1 Chemical composition of *P. nigrum* essential oils extracted by different methods.

No	Compounds	RI[a]	RI[b]	% GC				Method
				HDEO	MAEO	SCEO	HEEO	
1	α-thujene	925	924	0.1	–	–	–	RI, MS
2	α-pinene	932	931	7.1	4.8	2.2	1.6	RI, MS
3	Camphene	949	946	0.2	–	–	–	RI, MS
4	Sabinene	973	970	0.4	0.4	–	0.2	RI, MS
5	β-pinene	974	974	12.7	10.4	5.0	3.8	RI, MS
6	β-myrcene	988	988	2.5	2.1	1.1	0.8	RI, MS
7	α-phellandrene	1003	1002	5.2	2.7	2.1	1.6	RI, MS
8	3-carene	1010	1008	21.6	21.5	12.1	8.4	RI, MS
9	o-cymene	1026	1022	1.0	1.5	0.5	0.2	RI, MS
10	D-limonene	1030	1036	21.6	20.5	10.8	8.8	RI, MS
11	terpinolene	1090	1083	0.3	0.2	–	–	RI, MS
12	β-linalool	1095	1097	–	0.3	–	–	RI, MS
13	δ-3-elemene	1333	1333	1.5	1.1	4.6	3.1	RI, MS
14	α-cubebene	1349	1346	–	–	0.2	–	RI, MS
15	copaene	1376	1373	1.6	2.5	4.8	3.9	RI, MS
16	β-cubebene	1388	1386	0.2	0.2	0.6	0.5	RI, MS
17	β-elemene	1389	1388	0.3	0.5	0.8	0.8	RI, MS
18	β-caryophyllene	1418	1418	17.6	26.5	48.4	38.0	RI, MS
19	humulene	1452	1450	0.9	1.4	2.4	2.1	RI, MS
20	germacrene D	1480	1478	–	–	0.2	0.3	RI, MS
21	β-selinene	1483	1484	–	0.5	0.5	0.7	RI, MS
22	α-selinene	1494	1492	–	0.4	0.4	0.7	RI, MS
23	δ-cadinene	1519	1518	0.5	0.8	1.4	1.6	RI, MS
24	caryophyllene oxide	1578	1579	–	1.1	0.9	0.5	RI, MS
25	piperine	2933	2912	–	–	–	5.7	RI, MS
Class of substance:								
Monoterpenes				72.7	64.4	33.8	25.4	
Hydrocarbons				72.772.7	64.1	33.8	25.4	
Alcohols				–	0.3	–	–	
Sesquiterpenes				22.6	35.0	65.2	52.2	
Hydrocarbons				22.6	33.9	64.3	51.7	
EpoxyEpoxy				–	1.1	0.9	0.5	
Alkaloids				–	–	–	5.7	
Not identified				4.7	0.6	1.0	16.7	

[a] Retention index was collected from references (Adams, 2007).
[b] Retention index was calculated from the experimental data.

while the major volatile compounds in HEEO consist of β-caryophyllene (38.0%), d-limonene (8.8%), 3-carene (8.4%), piperine (5.7%), copaene (3.9%), β-pinene (3.8%), δ-3-elemene (3.1%), humulene (2.1%). *β*-Caryophyllene are known as a natural bicyclic sesquiterpene possessed many valuable bioactivities including anti-inflammatory and anti-cancer. The analysis shows that the method using supercriticial CO_2 is not only obtained very high content of β-caryophyllene but excluded piperine which is responsible for pungency of the pepper (Gorgani et al., 2017). Recently, supercriticial CO_2 extraction (Grinevicius et al., 2017) obtained different contents of β-caryophyllene (20.06–45.27%) depending on relative extraction conditions.

The major components of both MAEO and HDEO identified are monoterpenes. The volatile compounds of MAEO also showed a high content of β-caryophyllene (26.5%), 3-carene (21.5%) and d-limonene (20.5%), followed by β-pinene (10.4%), α-pinene (4.8%), α-phellandrene (2.7%) and copaene (2.5%). These compounds found in HDEO were d-limonene (21.6%), 3-carene (21.6%), β-caryophyllene (17.6%), β-pinene (12.7%), α-pinene (7.1%) and α-phellandrene (5.2%).

The previous report showed similarly major compositions including β-caryophyllene (13.0–33.4%), 3-carene (23.1–33.2%) and d-limonene (15.9–23.2%) from microwave-assisted extraction (Wang et al., 2018).

3.1.2. ^{1}H NMR analysis

Fig. 1 shows ^{1}H NMR spectra for all pepper essential oils. Similar signals are observed for each respective pairs of essential oils including HDEO and MAEO; SCEO and HEEO. Due to abundance of hydrocarbons in EOs, relative signals of all spectra are concentrated in resonance area of 0.5–2.5 ppm and 4.6–5.8 ppm which are respectively assigned to the methylene protons of saturated and unsaturated fatty chains and protons of double bond (C=C). These protons of β-caryophyllene presented in all EOs are observed at two intense peaks of 1.0 ppm and 5.1 ppm while *d*-limonene is found at two relative peaks of 1.7 ppm and 5.4 ppm (Grau and Mecking, 2013; Carbajal-Valdez et al., 2017). The intense peaks at 0.6 ppm and 1.6 ppm represented for protons of methyl groups in 3-carene molecule (Utenkova et al., 2017). Particularly, two samples, SCEO and HEEO appear some
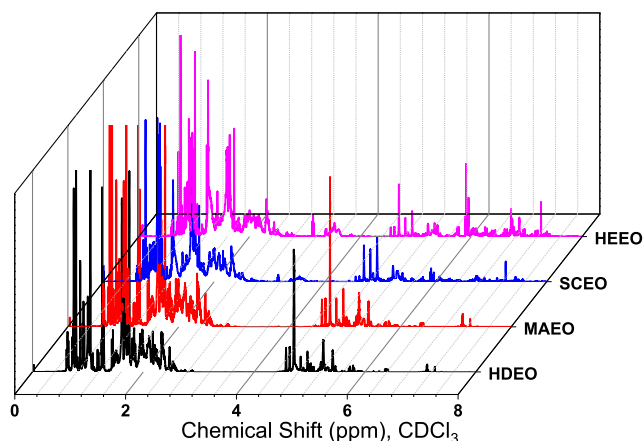
Fig. 1 ^{1}H NMR spectra (500 MHz, CDCl$_3$) of essential oils extracted by different methods.
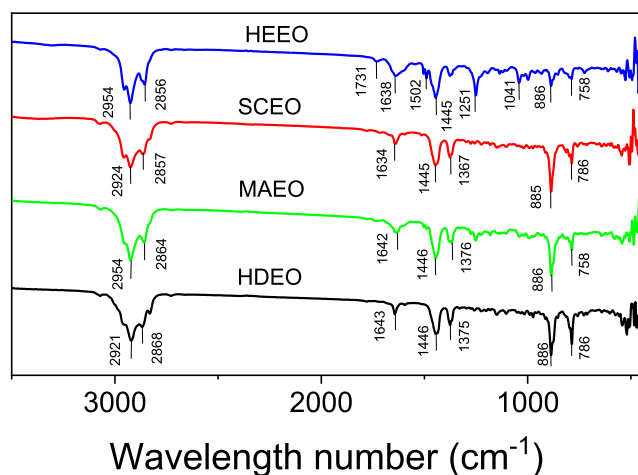

Fig. 2 FTIR spectra of essential oils extracted by different methods.

peaks at around 3.2–3.6 ppm and 6.0–7.5 ppm which characterize for methylene protons binding with specifically functional groups e.g. OH and NH, and protons of aromatic compounds, respectively (Hatzakis, 2019). This result reveals the presence of non-identifiable volatile compounds or/and non-volatile compounds which could not be identified by GC-MS method. It is clear that the extraction using solvents including supercritical CO$_2$ and hexane can destruct plant cell leading to release of many phytochemicals into the extraction solvent.

3.1.3. FTIR analysis

FTIR spectra for all oils are shown in Fig. 2. The typical absorption bands of the oils are similar, excepted in HEEO. The characteristic peaks at around 2960 and 2860 cm^{-1} are assigned to asymmetrical and symmetrical stretching vibrations of the aliphatic methylene groups. The hydrocarbons in all oils including β-caryophyllene, d-limonene, 3-carene, α-pinene, β-pinene and the others are characterized by intense bands at 1640 cm^{-1}, 1440 cm^{-1} and 885 cm^{-1} corresponding to stretching and bending vibrations of the C—C, C═C, and

C—H bonds, respectively (Tongnuanchan et al., 2012; Dang and Nguyen, 2019). In particular, although the volatile compositions of HEEO are not so different from the others (Table 1), some of the typical peaks appear in its spectrum. The sharp bands appearing at 1735 cm^{-1} and 1251 cm^{-1} respectively correspond to stretching vibration of carbonyl (C═O) and C—O groups relating esters of fatty acids and/or ketones that are well-dissolved in the hexane solvent during soaking process (Fleming and Williams, 2019). The peak at 1502 cm^{-1} associates to stretching vibration of aromatic rings that are also confirmed from ^{1}H NMR data.

3.1.4. UV–Vis spectroscopy

The UV–Vis spectra of pepper oils are shown in Fig. 3. The spectra of all extracted oils were measured using hexane as a solvent in the wavelength region of 200–400 nm. All oils show a broad absorbance peak in region of 245–300 nm which relates to the energy gap for π -π* transitions of double bond (C═C) in hydrocarbons. Both the oils, HDEO and MAEO show a maximum peak at 261 nm while the peak at 256 nm is observed for SCEO and HEEO. Moreover, the appearance of broad peaks in region of 315–390 nm is observed for both oils, SCEO and HEEO. It is assigned to the absorption of n-π* transitions in these oils. Two weak peaks at 338 and 352 nm can relate to aromatic compounds that cannot identify in the relative oils by GC-MS method. Additionally, value of absorbance at these peaks in HEEO is higher than the absorbance in SCEO, indicating that HEEO contains greater content of non-identifiable compounds which is confirmed from NMR and FTIR data.

3.1.5. Isothermal volatilization

Isothermal volatilization at room temperature is an important fragrant property for use of EOs as the scent essences. Proper understanding of the EO evaporation allows effective application of EO in the real life. Isothermal analysis of EO at room temperature can be evaluated by TGA measurement that investigates changes in the sample weight as a function of exposition time. In this study, the TGA measurement was car-
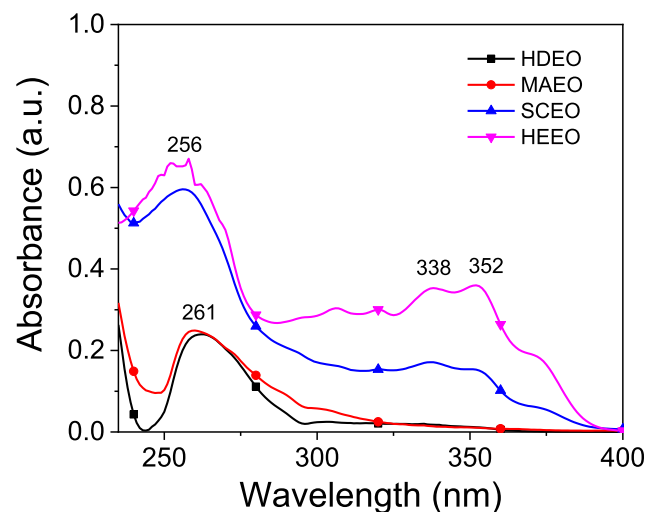

Fig. 3 UV–Vis spectra of essential oils extracted from different methods.

ried out at 27 °C for 2 h in air flow rate of 20 mL min^{-1}. The results are shown in Fig. 4. The TGA curves show that the weight loss is in range of 3.2–7.3% and it is dependent on the extraction of EO. Evaporation of SCEO is as low as 3.2% whereas the evaporation percentages of MAEO and HEEO are around 7.0%. Moreover, the evaporation behaviour of EOs is similar, excepted HEEO. TGA data of three the samples, HDEO, MAEO and SCEO showed a linear function of the weight loss according to exposition time which probably relates to zero order of the evaporation (Rosbrugh et al., 2000). The similar results have been observed in the previous reports on the other EOs (Le et al., 2020; Nguyen et al., 2018). Increase of evaporation rate is found in order of SCEO, HDEO and MAEO. Particularly, the weight loss rate of HEEO is observed as a quadratic function of time that showed a reaction order of the evaporation above zero. An exponential equation (R^2 = 99.99) found after fitting process is y = 7.65 *exp(-t/41.0) + 92.2; where y is loss weight; t is exposition time (min). The typical evaporation behaviour of HEEO can be because the presence of non-volatile molecules induces interruption with volatile molecules during evaporation process which may lead to the reaction order above zero. The evaporation of the pepper EOs is appreciably greater than *Cinnamomum cassia* EOs but lower than that of *Citrus microcarpa* EOs (Le et al., 2020; Nguyen et al., 2018).

3.1.6. Thermal behaviour

The thermal behaviour of EOs was evaluated by using simultaneous measurement of TGA and DSC in range of 30–500 °C at heating rate of 10 °C. The results are illustrated in Fig. 5 and the thermal data are listed in Table 2. The difference of thermal profiles is observed for the various oils. TGA curves of all samples showed that the thermal stability of all oils is above 70 °C and mass loss of 5% is around 115 °C. It allows the EOs used as a seasoning in the food technology with insignificant mass change. The difference of the thermal property is observed at region of high temperature (above 150 °C). The TGA curves of HDEO and MAEO showed a single stage of mass loss according to increase of heating temperature. The weight of HDEO (98.1%) and MAEO (96.8%) is almost completely lost at T_d values of 232 °C and 242 °C, respectively. The simultaneous DSC data showed the endothermic peaks of 180 °C for HDEO and 184 °C for MWEO that correspond
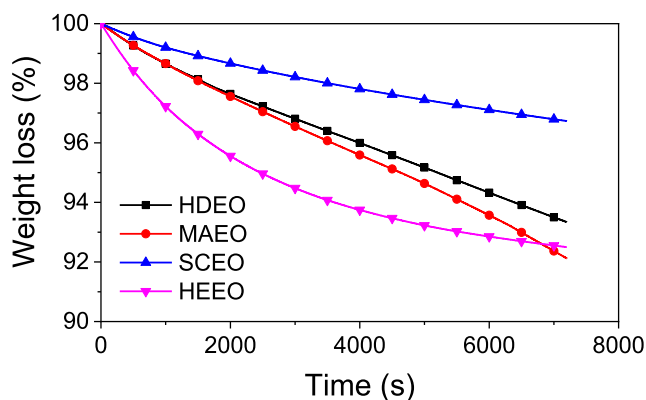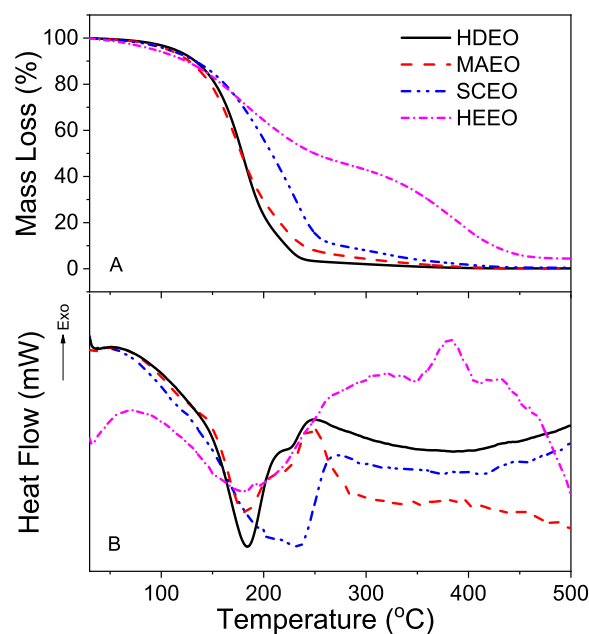

Fig. 5 Thermogravimetric analysis (A) and differential scanning calorimetry (B) of essential oils extracted from different methods.

Table 2 Profile of thermal behaviour, percent of mass loss and temperature peak for pepper oils.

Samples	Variables	Stages or Peaks[a]	
		First	Second
HDEO	T_d (°C)/m_{loss} (%)	70–232/98.1	–
	T_{DSC} (°C)	184 (endothermic)	–
MWEO	T_d (°C)/m_{loss} (%)	72–242/96.8	–
	T_{DSC} (°C)	180 (endothermic)	–
SCEO	T_d (°C)/m_{loss} (%)	70–251/85.1	251–410/14.4
	T_{DSC} (°C)	234 (endothermic)	
HEEO	T_d (°C)/m_{loss} (%)	70–258/48.1	258–460/47.2
	T_{DSC} (°C)	179 (endothermic)	381 (exothermic)

[a] T_d is decomposition temperature collected from TGA, m_{loss} is overall mass loss and T_{DSC} is temperature peak determined from DSC data.

Fig. 4 Isothermal property of essential oils using TGA measurement at 27 °C for 2 h.

to evaporation of relative EOs. The complete evaporation at the low temperature region reveals that these EOs abundantly contain the volatile compounds. Although T_d value of overall mass loss in SCEO (251 °C) is not so different comparing with the values of HDEO and MWEO, a slower mass loss process is obviously observed from TGA curve of CSEO. The half of sample weight loss at 217 °C is found for CSEO while the much lower temperature (~190 °C) are observed for both HDEO and MAEO. An endothermic peak at 234 °C found for SCEO can also relate to evaporation of the volatile com-

pounds in this EO. A special thermal profile of HEEO can be seen from Fig. 5. The mass loss of this EO with increasing heating temperature obviously occurs in two stages of TGA curve. Only 48.1% of sample weight lost in temperature region of 70–258 °C corresponds to an endothermic peak at 179 °C in the first stage. The second stage in temperature region of 258–460 °C with a loss weight of 47.2% relates to an exothermic peak at 381 °C which may be attributed to oxidation of organic compounds in the sample. The difference in thermal profiles among EOs can be because difference in their compositions of volatile and/or non-volatile compounds which is in agreement with ^{1}H NMR, FTIR and absorption analysis.

3.2. Influence of extractions on spent black pepper

3.2.1. Surface morphology

Raman and Gaikar (2002) reported the mechanism of piperine extraction from black pepper using hydrotropic compounds.
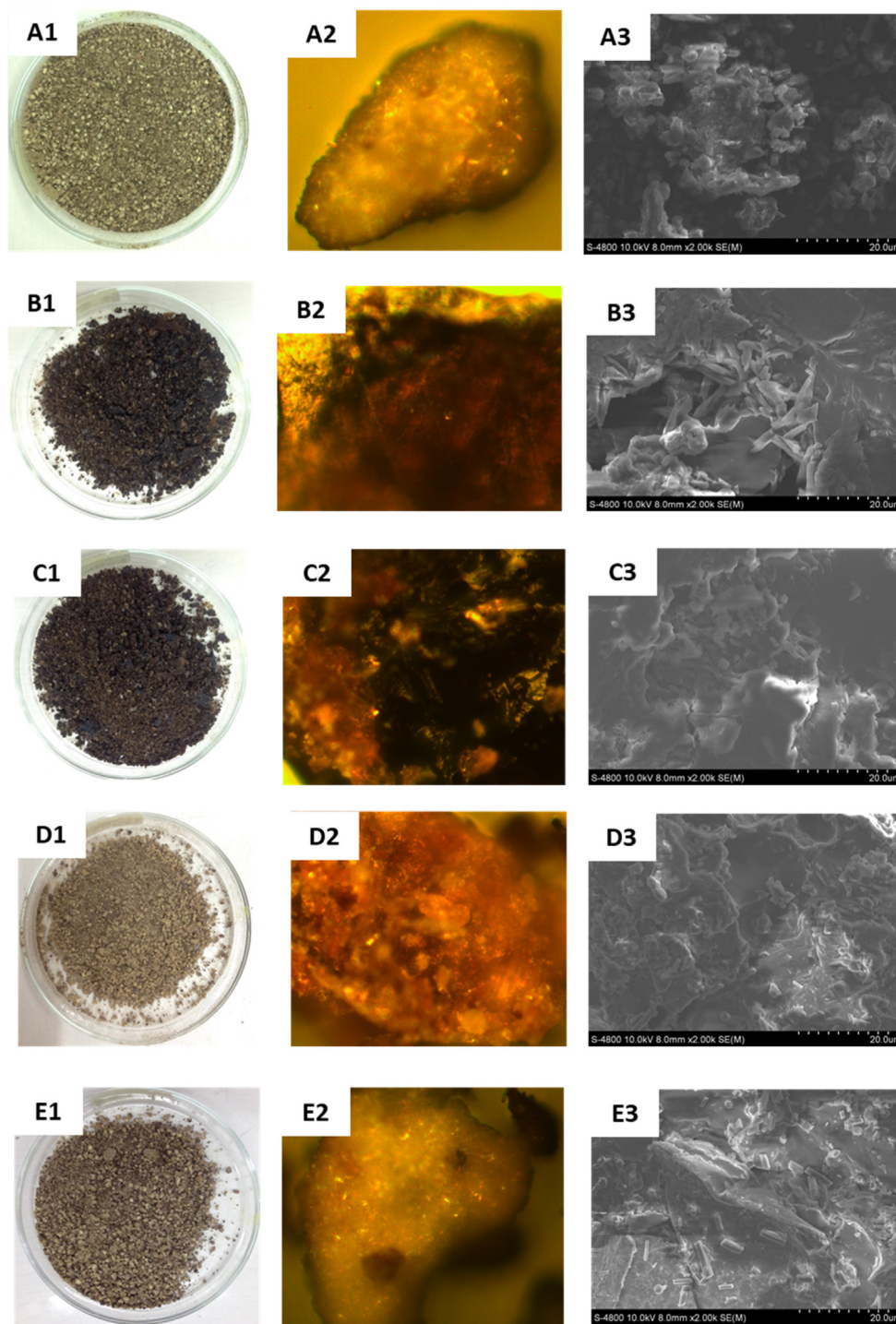

Fig. 6 Photos (left), microscopy (middle) and FE-SEM (right) images of the pre-extraction pepper (A1-A3), extraction by hydrodistillation (B1-B3), microwave-assisted hydrodistillation (C1-C3), supercritical CO_2 (D1-D3) and hexane (E1-E3).

They described that the solvent molecules disorganize the cellulosic cell wall after absorption process and then penetrate into the protein cell membrane, followed by release of piperine. Recently, Olalere et al. (2017) showed microwave irradiation ruptured the cell walls during oleoresin release from the black pepper. The mechanism of EO extraction can be investigated through studying surface morphology of the oil-spent black pepper. In the present work, all black peppers before and after extraction were investigated surface morphology using microscopy and SEM analysis. The images are shown in Fig. 6. The results revealed that all extraction methods induced obvious changes in the morphology of black pepper surface. Photos showed change in colors of oil-spent samples in comparison with the pre-extraction pepper. The HD and MA extractions induce black color on the pepper surface indicating carbonation by heating process which can be obviously observed in the microsopic images while the color and surface of black pepper are insignificantly changed in extraction using the solvents (Fig. 6D & 6E). The stone-like cells can be seen clearly from SEM igmages of pre-extraction black pepper (Fig. 6A3). The size of cells is found in range of 2–6 μm. The cell wall is almost completely destroyed under heating energy in both samples of HDBP and MABP. It also shows that the rupture capability by microwave irradiation is more remarkable than that of HD extraction. Under water penetration and application of heat, cellulose cell walls are swelled and different levels of pressure inside the cell led to the reduction of surface area. Although no changes in the surface of black pepper has been recognized from the microscope images of SCBP and HEBP, destruction of the cells still is observed from the respective SEM analysis as shown in Fig. 6D3 and E3 but it seems shape of the cells maintained after the release of essential oils into the solvents. Therefore, extraction using supercritical CO_2 and hexane as solvents showed operation manners different from using polar solvents and application of heating process.

3.2.2. Thermal properties of black peppers

To study extraction-dependent thermal properties of the spent black pepper, the pre-extraction and post-extraction solid samples were characterized by TGA measurement. The TGA curves of all peppers are shown in Fig. 7. The results showed that the thermal behaviour is slightly different among all sam-
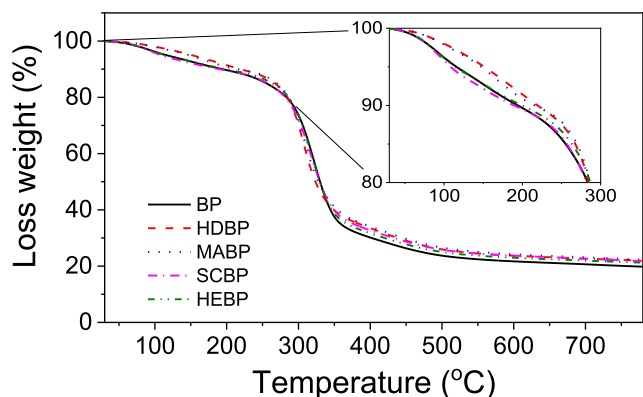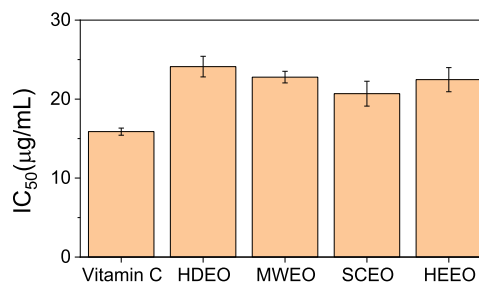

Fig. 8 DPPH radical scavenging activity of black pepper oils.

ples. The weight loss of HDBP and MABP slower than that of the pre-extraction sample in temperature range of 30–300 °C (inset of Fig. 7) confirmed their carbonation whereas thermal behavior of SCBP and HEBP is similar to pre-extraction black pepper, indicating unambiguous change in the structure of the black peppers. Moreover, the weight of ash remained after heat process of all the post-extraction samples are remarkably greater than solid ash of the pre-extraction sample. It reveals the good extraction yields of EO for all methods.

3.3. Antioxidant assay

Extraction-dependent antioxidant activity of black pepper essential oils is described in Fig. 8. The antioxidant assay based on DPPH radical scavenging method. The SCEO shows the highest activity with IC_{50} value of 20.7 ± 1.5 μg/mL, followed by HEEO (22.5 ± 1.5 μg/mL), MAEO (22.8 ± 0.7 μg/mL) and HDEO (24.1 ± 1.3 μg/mL). DPPH radical scavenging ability of these oils showed the better activity in comparison with previous reports (Jeena et al., 2014; Bagheri et al., 2014). Although the antioxidant activity of all oils slightly lower than vitamin C (15.9 ± 0.4 μg/mL), these EOs can be considered as an important natural source of antioxidant reagents.

3.4. Antibacterial assay

In order to study extraction-dependent antibacterial activity, all of the essential oils were tested against a Gram-negative, *E. coli* and a Gram – positive, *B. cereus*. The test environment and solvent (DMSO) were used as the negative control and ampicillin (1 mg mL^{-1}) was used as the positive control. The results showed that oils extracted by using solvents (SCEO and HEEO) did not exhibit anti-bacterial activity even used pure EOs whereas HDEO and MAEO exhibited high activity against the tested bacteria. Their antibacterial activity is plotted in Fig. 9 where the different concentrations of the samples (117, 137, 164, 205 μg mL^{-1}) are quantitatively determined by inhibition zones in millimeter. It shows that the different antibacterial activity between the EOs against the tested bacterial strains is found. MAEO showed the higher activity than HDEO in inhibition of *E. coli* but slightly lower in inhibition of *B. cereus*. It can be due to the difference in the structure of bacterial cell wall (Joe et al., 2011). Increase of inhibition zone according to the sample concentrations is observed for both bacterial strains and MIC values are found to be 137 μg mL^{-1} for both the essential oils. Therefore, the EOs

Fig. 7 TGA curves of pre-extraction black pepper (BP), extraction by hydrodistillation (HDBP), microwave-assisted hydrodistillation (MABP), supercritical CO_2 (CSBP) and hexane (HEBP).
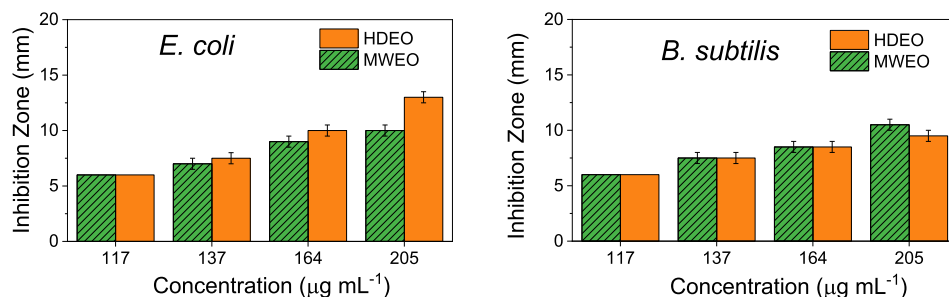
Fig. 9 Antibacterial activity of HDEO and MWEO against *E. coli* and *B. subtilis*.

in the present study exhibit higher activity in comparison with the recent reports (Tu et al., 2018; Gomez-Garcia et al., 2019).

3.5. Kinetics of non-isothermal decomposition

Because HDEO and MAEO, which are obtained from the most common extraction methods, showed similar chemical composition and physicochemical properties, MAEO was selected to investigate non-isothermal decomposition kinetics in the present work. Fig. 10 shows TGA and DTG curves described the conversional fractions and time derivative against the temperature increase at four different heating rates (10, 15, 20 and 25 °C min^{-1}). An apparent shift of TGA curves is attributed to the variation of heat flow rate inside the oil. Due to thermal lag within the oil, the higher heating rates may reduce the distribution of heat, led to the volatilization of oils at higher temperature region (Santos et al., 2011). The TGA curves show that the maximum conversional fractions take place rapidly in a temperature range of 400–500 K. A shift of temperature peaks toward the higher temperature zone with increase of heating rates is found in DTG curves which reveal
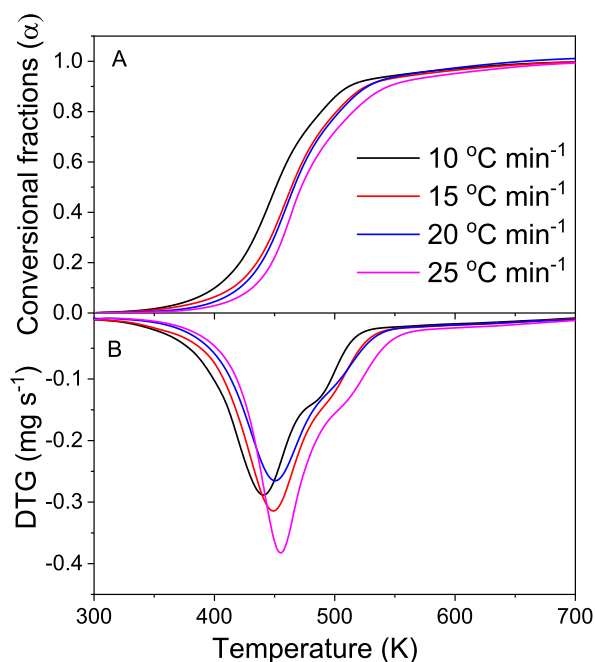
the reactions taken place more rapidly at the same time. Moreover, small shoulders relating to the conversion of EO in high temperatures is also observed in conversion fraction of 0.9. Thus, conversional fractions in range of 0.1–0.8 were used to evaluate the EO decomposition kinetic. Previous researches on the non-isothermal decomposition kinetic of solids (Chong et al., 2019; Cai et al., 2018) requested the conversional range of 0.2–0.7 to avoid inaccuracy due to DTG peak tail and the moisture evaporation of solid sample. In the present work, the volatilisation kinetic evaluation of the oil can be calculated from conversional fraction of 0.1.

The non-isothermal model free methods including two integral *iso*-conversional methods (FWO and KAS) and a differential *iso*-conversional method (Friedman) were utilized to determine activation energy of the non-isothermal decomposition via Eqs. (6), (7) and (9), respectively. Pre-exponential factors (A) of the non-isothermal decomposition were calculated via Kissinger method by using Eq. (10). The linear graphs for all methods are clearly observed in Fig. 11. High degree of parallelism at all conversional levels results average correlation coefficients of 0.948, 0.926 and 0.932 for FWO, KAS and Friedman, respectively (Table 3). The linearity demonstrated that these *iso*-conversional methods can be used to evaluate the non-isothermal kinetics of the oil.

Plots of E_α and A_α versus α are shown in Fig. 12. It is clear that values of E_a change along with different conversional fractions indicated a complex process with a multi-step mechanism during volatilisation of oil molecules. The lowest activation energy is found at $\alpha = 0.1$. It is steadily increased with values of α and achieved a maximum E_α at $\alpha = 0.6$ before decreasing again at high conversion fractions. The initial conversional fractions may relate to volatilisation of monoterpenes with low molecular weight such as α- and β-pinene. The increase of E_α is attributed to the evaporation of compounds with higher molecular weights while the decrease of E_α at high conversional fractions indicates exothermic process e.g. oxidation, competing the volatilisation process taken place in the oil. Appearance of an exothermic peak at 250 °C in the DSC data (Fig. 5B) confirms this competition.

Although trend of E_a versus α is similar for all three methods, the lowest values are found by Friedman method. KAS method shows the E_a of oil around 36.5–69.7 KJ mol^{-1} while these values found from FWO and Friedman methods are in higher range of 41.2–73.7 KJ mol^{-1} and 40.2–73.6 KJ mol^{-1}, respectively. Mean E_a values are found in a decreasing order of FWO (64.3 KJ mol^{-1}), Friedman (63.9 KJ mol^{-1}) and KAS (60.0 KJ mol^{-1}). It should be noted that at low conversional fractions the E_a value of Friedman method is slightly

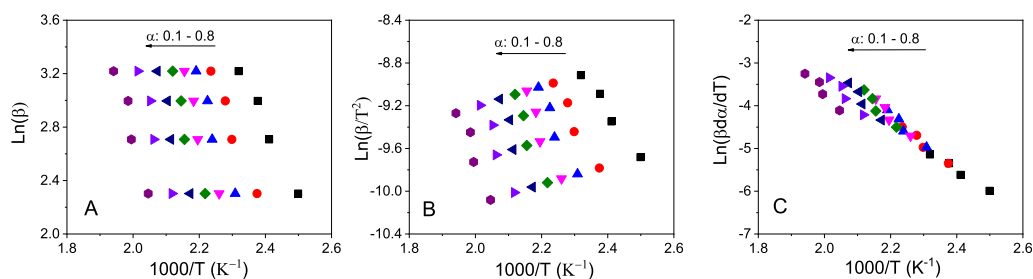**Fig. 10** TGA (A) and DTG (B) curves of MAEO at four different heating rates.

Fig. 11 Plots of *iso*-conversional methods for MAEO: Flynn–Wall–Ozawa (A) and Kissinger–Akahira–Sunose (B), and Friedman (C).

Table 3 Values of activation energy, pre-exponential factor and correlation coefficient according to conversion fractions for all kinetic models of MAEO.

α	FWO			KAS			Friedman		
	E_a (kJ mol^{-1})	A (s^{-1})[a]	R^2	E_a (kJ mol^{-1})	A (s^{-1})[a]	R^2	E_a (kJ mol^{-1})	A (s^{-1})[a]	R^2
0.1	41.2	1.99×10^4	0.980	36.5	4.98×10^3	0.972	40.3	1.50×10^4	0.978
0.2	52.9	5.67×10^5	0.960	48.4	1.59×10^5	0.947	51.9	4.30×10^5	0.952
0.3	61.7	6.91×10^6	0.942	57.6	2.13×10^6	0.927	61.9	7.19×10^6	0.935
0.4	68.6	4.75×10^7	0.931	64.6	1.57×10^7	0.916	68.6	4.77×10^7	0.922
0.5	73.1	1.66×10^8	0.919	69.2	5.66×10^7	0.901	73.2	1.69×10^8	0.910
0.6	73.7	1.97×10^8	0.935	69.7	6.45×10^7	0.920	73.6	1.92×10^8	0.925
0.7	71.9	1.19×10^8	0.935	67.6	3.56×10^7	0.920	71.8	1.15×10^8	0.925
0.8	71.0	9.26×10^7	0.925	66.3	2.52×10^7	0.905	70.2	7.42×10^7	0.915
Mean	64.3	7.87×10^7	0.948	60.0	2.50×10^7	0.926	63.9	7.57×10^7	0.932

[a] Values of A calculated for heating rate at 10 °C min^{-1}.
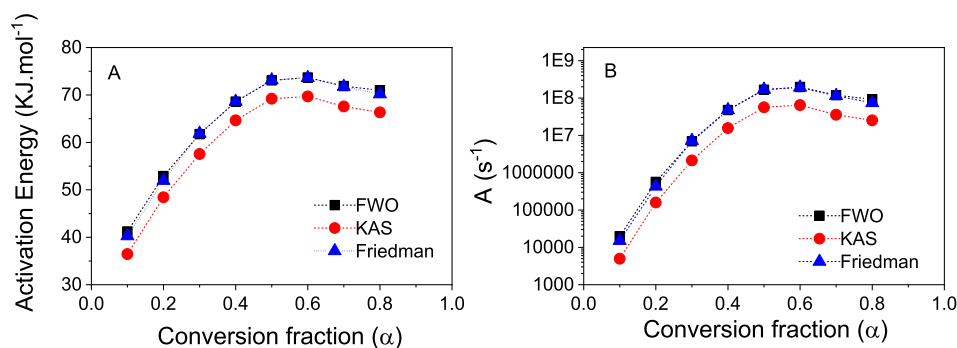

Fig. 12 Plots of activation energy (A) and pre-exponential factor (B) versus conversional fractions of MAEO.

lower than that of FWO but it becomes slightly higher in the high conversional fractions while the E_a trend of KAS and FWO methods is similar for entire conversion process. The difference in trend of E_a obtained from Friedman method compared with both integral methods is due to their relating mathematical models where Friedman analysis adopts via differential method (Eq. (9)) while both integral methods based on the assumption of temperature integral. The E_a of pepper oil is very similar to *C. cassia* oils and biodiesels (50–70 KJ mol^{-1}) however it is much lower than that of palm oils (170–180 KJ mol^{-1}) (Le et al., 2020; Santos et al., 2014; Oliveira et al., 2013). It may relate to difference in evaporation point of their main compounds.

The values of A_α are derived by substitution of relating E_a values into equation of Kissinger method (Eq. (11)). Thus, the A_α vs α dependence is similar to the E_a trend. Values of A_α at heating rate of 10 °C min^{-1} for all methods are found in range of 4.98×10^3–1.97×10^8 s^{-1} in entire conversional levels. The broad change of A values can be attributed to the complex decomposition of the oil. The lowest A value found at α = 0.1 indicates a system with less reactivity which is attributed to collision of oil molecules on the surface. Increase of A values with high conversional fractions reveals increasing interaction among the molecules. It is a fact that evaporation of compounds with great molecular weights involves many more complex progress including collisions and breakdown/ decomposition of molecules in the oil.

4. Conclusion

The EOs of black pepper were extracted by four different methods which confirmed as an important factor influencing the physicochemical properties of the oils. The extract using solvents showed the higher yields compared to the others. A total of 25 volatile compounds including monoterpene and sesquiterpene hydrocarbons was identified by GC-MS technique. The essential oils extracted by using solvents possessed the high non-volatilisable compositions which were obviously demonstrated by ^{1}H NMR, FTIR, UV–Vis and TGA technique. The evaporation of all essential oils was in range of 3.2–7.3% at 27 °C. For studies on the spent black peppers, the extractions using the solvents showed operation manners different from the extractions using heating process. Both HDEO and MAEO were found to exhibit the highest antibacterial activity. Due to low-cost and rapid extraction, microwave technique possesses potential applications for preparation of black pepper EO. The isoconversional methods showed an appropriate model to study non-isothermal decomposition kinetics of the black pepper essential oil. The activation energy and pre-exponent factor of non-isothermal decomposition were calculated by four different kinetic models. The kinetic parameters were found to be in range of 36.5–73.7 KJ mol^{-1} for the activation energy and 4.98×10^3–1.97×10^8 s^{-1} for pre-exponent factors.

Declaration of Competing Interest

The authors declare that they have no known competing financial interests or personal relationships that could have appeared to influence the work reported in this paper.

Acknowledgement

Appendix A. Supplementary material

Antibacterial activity images of oils extracted by hydrodistillation and microwave-assisted hydrodistillation are available electronically from website or from the corresponding author on request. Supplementary data to this article can be found online at https://doi.org/10.1016/j.arabjc.2020.08.008.

References

Adams, R.P., 2007. Identification of Essential Oil Components by Gas Chromatography/Mass Spectrometry. Allured publ, Corp, Carol stream, IL.

Akahira, T., Sunose, T., 1971. Method of determining activation deterioration constant of electrical insulating materials. Res. Rep. Chiba Inst. Technol. (Sci. Technol.) 16, 22–31.

Ahmad, N., Fazal, H., Abbasi, B.H., Farooq, S., Ali, M., Khan, M.A., 2012. Biological role of Piper nigrum L. (black pepper): A review. Asian Pacific J. Trop. Biomed. 2, S1945–S1953. https://doi.org/10.1016/S2221-1691(12)60524-3.

Bagheri, H., Manap, M.Y.B.A., Solati, Z., 2014. Antioxidant activity of Piper nigrum L. essential oil extracted by supercritical CO$_2$ extraction and hydrodistillation. Talanta 121, 220–228. https://doi.org/10.1016/j.talanta.2014.01.007.

Bakha, M., Mtili, N.E., Machon, N., Aboukhalid, K., Amchra, F.Z., Khiraoui, A., Gibernau, M., Tomi, F., Faiz, C.A., 2020. Intraspecific chemical variability of the essential oils of Moroccan endemic Origanum elongatum L. (Lamiaceae) from its whole natural habitats. Arab. J. Chem. 13, 3070–3081.

Bakkali, F., Averbeck, S., Averbeck, D., Idaomar, M., 2008. Biological effects of essential oils – A review. Food Chem. Toxicol. 46, 446–475.

Baptista-Silva, S., Borges, S., Ramos, O.L., Pintado, M., Bruno Sarmento, 2020. The progress of essential oils as potential therapeutic agents: a review, doi:10.1080/10412905.2020.1746698.

Cai, J., Xu, D., Dong, Z., Yu, X., Yang, Y., Banks, S.W., Bridgwater, A.V., 2018. Processing thermogravimetric analysis data for isoconversional kinetic analysis of lignocellulosic biomass pyrolysis: Case study of corn stalk. Renew. Sustain. Energy Rev. 82, 2705–2715. https://doi.org/10.1016/j.rser.2017.09.113.

Carbajal-Valdez, R., Jiménez-Pérez, J.L., Cruz-Orea, A., Correa-Pacheco, Z.N., Alvarado-Noguez, M.L., Romero-Ibarra, I.C., Mendoza-Alvarez, J.G., 2017. Thermal properties of centrifuged oils measured by alternative photothermal techniques. Thermochimca Acta 657, 66–7167. https://doi.org/10.1016/j.tca.2017.09.014.

Chong, C.T., Mong, G.R., Ng, J.H., Chong, W.W.F., Ani, F.N., Lam, S.S., Ong, H.C., 2019. Pyrolysis characteristics and kinetic studies of horse manure using thermogravimetric analysis. Energy Convers. Manage. 180, 1260–1267. https://doi.org/10.1016/j.enconman.2018.11.071.

Dang, C.H., Nguyen, T.D., 2019. Physicochemical characterization of Robusta coffee ground spent oil for biodiesel manufacturing. Waste Biomass Valorization 10, 2703–2712. https://doi.org/10.1007/s12649-018-0287-9.

Doyle, C.D., 1962. Estimating isothermal life from thermogravimetric data. J. Appl. Polym. Sci. 6, 639–642. https://doi.org/10.1002/app.1962.070062406.

Fleming, I., Williams, D., 2019. Infrared and Raman Spectra. In: Spectroscopic Methods in Organic Chemistry. Springer, Cham, pp. 85–121.

Flynn, J.H., 1997. The «temperature integral»-its use and abuse. Thermochi. Acta 300, 83–92. https://doi.org/10.1016/S0040-6031(97)00046-4.

Freitas, I.R., Cattelan, M.G., 2018. Chapter 15 - Antimicrobial and antioxidant properties of essential oils in food systems—an overview. In: Holban, A.M., Grumezescu, A.M. (Eds.), Microbial Contamination and Food Degradation. São Paulo State University, São José do Rio Preto, São Paulo, Brazil, pp. 443–470.

Friedman, H.L., 1964. Kinetics of thermal degradation of char-forming plastics from thermogravimetry. Application to a phenolic plastic. J. Polym. Sci. Part C: Polym. Symposia 6, 183–195. https://doi.org/10.1002/polc.5070060121.

Gomez-Garcia, M., Sol, C., de Nova, P.J.G., Puyalto, M., Mesas, L., Puente, H., Mencia-Ares, O., Miranda, R., Arguello, H., Rubio, P., Carvajal, A., 2019. Antimicrobial activity of a selection of organic acids, their salts and essential oils against swine enteropathogenic bacteria. Porcine Health Manage. 5, 32. https://doi.org/10.1186/s40813-019-0139-4.

Gorgani, L., Mohammadi, M., Najafpour, G.D., Nikzad, M., 2017. Piperine—The bioactive compound of black pepper: from isolation to medicinal formulations. Compr. Rev. Food Sci. Food Saf. 16, 124–140. https://doi.org/10.1111/1541-4337.12246.

Grau, E., Mecking, S., 2013. Polyterpenes by ring opening metathesis polymerization of caryophyllene and humulene. Green Chem. 15, 1112–1115. https://doi.org/10.1039/C3GC40300A.

Grinevicius, V.M.A.S., Andrade, K.S., Ouriquea, F., Micke, G.A., Ferreira, S.R.S., Pedrosa, R.C., 2017. Antitumor activity of conventional and supercritical extracts from Piper nigrum L. cultivar Bragantina through cell cycle arrest and apoptosis induction. J. Supercrit. Fluids 128, 94–101. https://doi.org/10.1016/j.supflu.2017.05.009.

Hatzakis, E., 2019. Nuclear Magnetic Resonance (NMR) Spectroscopy in Food Science: A Comprehensive Review. Compr. Rev. Food Sci. Food Saf. 18, 189–220. https://doi.org/10.1111/1541-4337.12408.

Hoerr, C.W., Harwood, H.J., 1951. Solubilities of high molecular weight aliphatic compounds in n-hexane. J. Org. Chem. 16, 779–791. https://doi.org/10.1021/jo01145a020.

Jaramillo, M.A., Manos, P.S., 2001. Phylogeny and patterns of floral diversity in the genus *Piper* (Piperaceae). Am. J. Bot. 88, 706–716. https://doi.org/10.2307/2657072.

Jeena, K., Liju, V.B., Umadevi, N.P., Kuttan, R., 2014. Antioxidant, Anti-inflammatory and Antinociceptive Properties of Black Pepper Essential Oil (*Piper nigrum* Linn). J. Essential Oil Bearing Plants 17, 1–12. https://doi.org/10.1080/0972060X.2013.831562.

Joe, J., Sivalingam, P., Siva, D., Kamalakkannan, S., Anbarasu, K., Sukirtha, R., Krishnan, M., Achiraman, S., 2011. Comparative evaluation of antibacterial activity of silver nanoparticles synthesized using *Rhizophora apiculata* and glucose. Colloids Surfaces B: Biointerfaces 88, 134–140. https://doi.org/10.1016/j.colsurfb.2011.06.022.

Kaefer, C.M., Milner, J.A., 2008. The role of herbs and spices in cancer prevention. J. Nutrit. Biochem. 19 (6), 347–361. https://doi.org/10.1016/j.jnutbio.2007.11.003.

Kamble, V.A., Patil, S.D., 2008. Spice-derived essential oils: Effective antifungal and possible therapeutic agents. J. Herbs Spices Med Plants 14, 129–143. https://doi.org/10.1080/10496470802598677.

Le, V.D., Tran, V.T., Dang, V.S., Nguyen, D.T., Dang, C.H., Nguyen, T.D., 2020. Physicochemical characterizations, antimicrobial activity and non-isothermal decomposition kinetics of *Cinnamomum cassia* essential oils. J. Essent. Oil Res. 32, 158–168. https://doi.org/10.1080/10412905.2019.1700834.

Li, Y.-X., Zhang, C., Pan, S., Chen, L., Liu, M., Yang, K., Zeng, X., Tian, J., 2020. Analysis of chemical components and biological activities of essential oils from black and white pepper (*Piper nigrum* L.) in five provinces of southern China. LWT 117 (108644). https://doi.org/10.1016/j.lwt.2019.108644.

Meghwal, M., Goswami, T.K., 2013. Piper nigrum and Piperine: An Update. Phytother. Res. 27, 1121–1130. https://doi.org/10.1002/ptr.4972.

Murray, P., White, J., 1955. Kinetics of the thermal dehydration of clays. Part IV. Interpretation of the differential thermal analysis of the clay minerals. Trans. J. British Ceramic Soc. 54, 204–238.

Nguyen, T.N.T., Huynh, T.N.N., Tran, V.T., Dang, C.H., Hoang, T.K.D., Nguyen, T.D., 2018. Physicochemical characterization, bioactivity evaluation of essential oil from *Citrus microcarpa* Bunge flower and leaf. J. Essent. Oil Res. 30 (4), 285–292. https://doi.org/10.1080/10412905.2018.1435428.

Nisha, P., Singhal, R.S., Pandit, A.B., 2009. The degradation kinetics of flavor in black pepper (*Piper nigrum* L.). J. Food Eng. 92, 44–49. https://doi.org/10.1016/j.jfoodeng.2008.10.018.

Olalere, O.A., Abdurahman, N.H., Alara, O.R., 2017. Extraction, radical scavenging activities and physicochemical fingerprints of black pepper (*Piper nigrum*) extract. J. Food Meas. Charact. 11, 2195–2201. https://doi.org/10.1007/s11694-017-9604-4.

Oliveira, L.E., Giordani, D.S., Paiva, E.M., De Castro, H.F., Silva, M.L.C.P.D., 2013. Kinetic and thermodynamic parameters of volatilization of biodiesel from babassu, palm oil and mineral diesel by thermogravimetric analysis (TG). J. Therm. Anal. Calorim. 111, 155–160. https://doi.org/10.1007/s10973-011-2163-8.

Peng, C., Liu, H., Hu, Y., 2001. Solid–liquid equilibria based on an equation of state for chain fluids. Fluid Phase Equilib. 180, 299–311. https://doi.org/10.1016/S0378-3812(01)00369-7.

Perakis, C., Louli, V., Magoulas, K., 2005. Supercritical fluid extraction of black pepper oil. J. Food Eng. 71, 386–393. https://doi.org/10.1016/j.jfoodeng.2004.10.049.

Raman, G., Gaikar, V.G., 2002. Extraction of piperine from *Piper nigrum* (black pepper) by hydrotropic solubilization. Ind. Eng. Chem. Res. 41, 2966–2976. https://doi.org/10.1021/ie0107845.

Rueda-Ordóñez, Y.J., Tannous, K., 2015. Isoconversional kinetic study of the thermal decomposition of sugarcane straw for thermal conversion processes. Bioresour. Technol. 196, 136–144. https://doi.org/10.1016/j.biortech.2015.07.062.

Rosbrugh, I.M., Nishimura, S.Y., Nishimura, A.M., 2000. Evaporation kinetics in short-chain alcohols by optical interference. J. Chem. Educ. 77, 1047. https://doi.org/10.1021/ed077p1047.

Sangha, J.S., Astatkie, T., Cutler, G.C., 2017. Ovicidal, larvicidal, and behavioural effects of some plant essential oils on diamondback moth (Lepidoptera: Plutellidae). Can. Entomol. 149, 639–648. https://doi.org/10.4039/tce.2017.13.

Santos, A.G.D., Caldeira, V.P.S., Farias, M.F., Araújo, A.S., Souza, L.D., Barros, A.K., 2011. Characterization and kinetic study of sunflower oil and biodiesel. J. Therm. Anal. Calorim. 106, 747–751. https://doi.org/10.1007/s10973-011-1838-5.

Santos, A.G.D., Araujo, A.S., Caldeira, V.P.S., Fernandes, V.J., Souza, L.D., Barros, A.K., 2014. Kinetic study and thermoxidative degradation of palm oil and biodiesel. Thermochim. Acta 592, 18–22. https://doi.org/10.1016/j.tca.2014.08.006.

Tongnuanchan, P., Benjakul, S., Prodpran, T., 2012. Properties and antioxidant activity of fish skin gelatin film incorporated with citrus essential oils. Food Chem. 134, 1571–1579. https://doi.org/10.1016/j.foodchem.2012.03.094.

Tran, T.H., Ha, L.K., Nguyen, D.C., Dao, T.P., Nhan, L.T.H., Nguyen, D.H., Nguyen, T.D., Vo, D.V.N., Tran, Q.T., Bach, L.G., 2019. The study on extraction process and analysis of components in essential oils of black pepper (*Piper nigrum* L.) seeds harvested in Gia Lai Province, Vietnam. Processes 7, 56.

Tu, X.-F., Hu, F., Thakur, K., Li, X.-L., Zhang, Y.-S., Wei, Z.-J., 2018. Comparison of antibacterial effects and fumigant toxicity of essential oilsextracted from different plants. Ind. Crops Prod. 124, 192–200.

Utenkova, D.B., Skakovskii, E.D., Senkov, G.M., Agabekov, V.E., Baranovskii, A.V., Bogushevich, S.E., Sidorenko, A.Y., 2017. NMR and GC analyses of 3-carene isomerization products over activated glauconite. J. Appl. Spectrosc. 83, 1026–1030.

Wang, Y., Li, R., Jiang, Z.T., Tan, J., Tang, S.H., Li, T.T., Liang, L.L., He, H.J., Liu, Y.M., Li, J.T., Zhang, X.C., 2018. Green and solvent-free simultaneous ultrasonic-microwave assisted extraction of essential oil from white and black peppers. Ind. Crops Prod. 114, 164–172.

Zhao, C., Yang, X., Tian, H., Yang, L., 2020. An improved method to obtain essential oil, flavonols and proanthocyanidins from fresh *Cinnamomum japonicum* Sieb. leaves using solvent-free microwave-assisted distillation followed by homogenate extraction. Arab. J. Chem. 13, 2041–2052.